

Article

# Novel H6 Transformerless Inverter for Grid Connected Photovoltaic System to Reduce the Conduction Loss and Enhance Efficiency

Aditi Atul Desai <sup>1,\*</sup>, Suresh Mikkili <sup>1,\*</sup>  and Tomonobu Senjyu <sup>2,\*</sup> 

<sup>1</sup> Electrical and Electronics Engineering Department, National Institute of Technology, Ponda 403401, India; aditi@gec.ac.in

<sup>2</sup> Department of Electrical and Electronics Engineering, University of Ryukyus, Okinawa 903-0213, Japan

\* Correspondence: mikkili.suresh@nitgoa.ac.in (S.M.); b985542@tec.u-ryukyu.ac.jp (T.S.)

**Abstract:** Presence of a transformer in a grid connected photovoltaic system provides galvanic isolation between the photovoltaic panels and the grid. However, it increases the overall cost, makes the circuit bulky and reduces the efficiency of the system. Hence, transformerless inverters have gained significant importance owing to its low cost, light weight and increased efficiency. However, due to the absence of the transformer, there is no galvanic isolation between photovoltaic panels and the grid and there is always a threat of flow of leakage current. In this research paper, an elaborate analysis of H4, H5 and H6 transformerless inverter is carried out. DC side decoupled circuits are studied to eliminate the leakage current. Their performances are compared based on the simulations carried out in MATLAB/SIMULINK software. A novel H6 inverter is proposed by introducing an additional switch in H5 topology. A direct current path is provided in H5 topology during one of the active modes, so that current flows through few switches thereby reducing the conduction losses. Common mode voltage remains constant in the proposed H6 inverter and hence the leakage current is eliminated. The proposed H6 inverter can thus be a promising topology to eliminate leakage current and reduce conduction loss in the transformerless grid connected photovoltaic system.

**Keywords:** transformerless inverter; leakage current; common mode voltage; parasitic capacitance



**Citation:** Desai, A.A.; Mikkili, S.; Senjyu, T. Novel H6 Transformerless Inverter for Grid Connected Photovoltaic System to Reduce the Conduction Loss and Enhance Efficiency. *Energies* **2022**, *15*, 3789. <https://doi.org/10.3390/en15103789>

Academic Editor: Luis Hernández-Callejo

Received: 7 April 2022  
Accepted: 19 May 2022  
Published: 21 May 2022

**Publisher's Note:** MDPI stays neutral with regard to jurisdictional claims in published maps and institutional affiliations.



**Copyright:** © 2022 by the authors. Licensee MDPI, Basel, Switzerland. This article is an open access article distributed under the terms and conditions of the Creative Commons Attribution (CC BY) license (<https://creativecommons.org/licenses/by/4.0/>).

## 1. Introduction

In today's ever growing energy demand all over the world, photovoltaics (PV) are playing a pivotal role in catering this demand as a source of renewable energy. Solar energy is available in abundance for free and is a clean source of energy. Thus, it is gaining popularity compared to other renewable energy sources. Due to the latest advancements in PV technology, the cost of mass scale production of PV has considerably reduced. Secondly, the government incentives and subsidies offered on PV panels is responsible for its wide usage. PV converts solar energy into DC electrical energy. However, when connecting to the grid, a well-designed DC to AC converter is required for safe and reliable operation to extract maximum efficiency from solar panels. Grid connected PV systems are classified based on the presence of a transformer and absence of a transformer [1]. The presence of a transformer offers galvanic isolation between the PV and the grid. Hence, leakage current is absent and there is no injection of DC current into the grid. However, the inclusion of a transformer makes the circuit heavy, bulky and costly. The overall efficiency of the PV system also reduces due to the presence of a transformer. Hence, the concept of a transformerless grid connected PV system has come into existence. They are light in weight, small in size and are less expensive. They also give improved efficiency compared to a grid connected PV system with a transformer. However, they suffer from a major drawback of not providing galvanic isolation. There is a safety concern due to the flow of high leakage current from the PV to the grid as shown in Figure 1 [2].

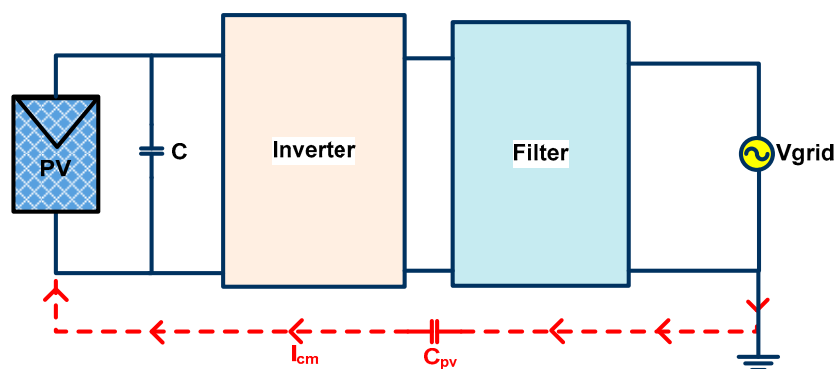


**Figure 1.** Leakage current path in a transformerless inverter.

Stray capacitance or parasitic capacitance ( $C_{pv}$ ) is formed in transformerless system due to the variation in the potential between PV and ground. This variation in potential is called common mode voltage ( $V_{cm}$ ). The factors affecting stray capacitance are dust and humidity, surface of PV and grounded frame, distance between PV cell and module [3]. The parasitic capacitance is charged and discharged by common mode voltage which gives rise to leakage current or common mode current ( $I_{cm}$ ). This leakage current, not only poses a threat to the safety of the personnel handling the PV but also increases the current ripples in the grid, electromagnetic interference and overall system losses. Hence, transformerless inverters for a grid connected PV system should strictly adhere to the safety standards such as IEEE 1547.1, VDE0126-1-1, IEC61727, EN 50106 and AS/NZS5033 [3]. Consequently, many researchers have suggested methods to eliminate the leakage current such as AC side decoupling, DC side decoupling, using common ground configurations or clamping the common mode voltage [4].

Roberto Gonzalez et al. [5] proposed a new transformerless PV inverter with six switches and two diodes. They concluded that the proposed topology generated constant common mode voltage, exhibited high efficiency and could operate at any power factor. S. V. Araujo et al. [6] reviewed many existing transformerless inverters and proposed a new inverter composed of the association of two step-down converters. The circuit was evaluated experimentally to achieve high efficiency with an optimized semiconductor configuration. Tamas Kerekes et al. [7] introduced HB-ZVR topology to give an alternate solution for bidirectional switch. Many researchers carried out a review of transformerless inverter topologies for single-phase grid connected photovoltaic systems [8–14]. Li Zang et al. [15] proposed positive neutral point clamped cell and the negative neutral point clamped cell for the grid tied inverter topology. Zameer Ahmed et al. [16] proposed improved H6 common mode voltage clamped topology with altered modulation strategy. Monirul Islam et al. [17] introduced H6 type inverter to inject reactive power into the grid. T.K.S. Freddy et al. [18] proposed modulation strategies to provide bidirectional current path during freewheeling period. Reactive power control is attained in H5 and HERIC inverters with proposed modulation strategy. H. Albalawi et al. [19] recommended improved H5 topology with a boost converter to operate in continuous conduction mode to guarantee MPPT conditions. A. Anurag et al. [20] proposed an integrated dc-dc converter-based transformerless PV inverter connected to the grid. It aims at maintaining high efficiency, even if the PV array voltage falls below the peak value of grid voltage. S.K.Kuncham et al. [21] proposed a new arrangement of single-phase two-stage hybrid transformerless multilevel inverter for PV system. The proposed multilevel inverter is derived from a combination of a half bridge, bidirectional switches and a diode clamped branch. Hong Li et al. [22] introduced H5-D topology as an improvement to H5 topology by adding a clamping diode. The two topologies are experimentally validated and confirmed the advantages of the proposed topology. Yam P. Siwakoti et al. [23] proposed a family of flying capacitor transformerless inverters for single-phase PV system. It only needs four power switches and/or diodes, one capacitor and a small filter at the output stage. M.Xu et al. [24] introduced a new

H6-type inverter to ensure that the current flows through a fewer number of switches in the active mode as compared to the H5 inverter. B. Yang et al. [25] added two symmetrical switches on the DC side of the H5 topology to eliminate the leakage current. The authors successfully operated the inverter with unipolar SPWM and double frequency SPWM control strategy. Li Zang et al. [26] have compared the performances of H5 and Heric along with the proposed family of H6 transformerless inverter topologies. A universal prototype is built to evaluate their performances in terms of leakage currents and efficiency. A. Datta et al. [27] have designed a circuit using an additional branch so as to clamp the potential of the freewheeling path to half the input voltage in the freewheeling period. This guarantees that there is no fluctuating common mode voltage in the unipolar SPWM full-bridge inverter. K.S. Kumar et al. [28] proposed a bidirectional clamping (BDC)-based H5, Heric and H6 transformerless inverter topologies with improved PWM schemes. BDC branch reduced the leakage current and the improved PWM modulation confirmed the bidirectional current path while operating in the negative power region. S. Ahmad et al. [29] developed a novel single-phase transformerless topology using MOSFETs and SiC diodes as no reverse recovery issues are required for the main power switches. Two additional switches and two diodes with the H4 inverter ascertain that the PV module is disconnected from the grid during the freewheeling mode. M.A. Gaafar et al. [30] reviewed common-ground photovoltaic inverters to eliminate the leakage current produced due to the stray capacitances in PV systems.

From the above literature survey, it can be seen that some researchers have compared the performances of DC-decoupled inverters with AC-decoupled inverters. Some researchers are still trying to invent new topologies and modulation techniques to reduce the leakage current, conduction losses and thereby increase the overall efficiency of single phase transformerless inverter connected to the grid. There is also ample scope to compare conventional H bridge inverter with existing DC-decoupled transformerless inverters such as H5 and H6 inverters. Owing to the above fact, in this research paper, an elaborate analysis of full-bridge inverter is carried out and its performance is compared with H5 and family of H6 inverters. Common mode voltage, leakage current, conduction losses and efficiency are the parameters considered for comparison. An effort is made to overcome the shortcomings of the H5 inverter such as high conduction loss, reduced efficiency by introducing a novel H6 inverter concept. A novel H6 inverter topology is proposed with improved modulation strategy to nullify the fluctuations in common mode voltage and to eliminate the leakage current. The proposed inverter is a modification to the existing H5 inverter, with an additional switch between the negative terminal of the DC supply and the first leg of the H bridge. This structure guarantees that only two switches are turned on during the active mode of negative half cycle of the grid voltage. This strategy confirms that the conduction loss of novel H6 inverter is reduced compared to H5 and H6 inverters. The modulation strategy adopted for this inverter confirms that the common mode voltage is maintained constant thereby drastically reducing the leakage current as compared to H5 and H6 inverter. All the simulations in this research paper are carried out in MATLAB/Simulink software.

## 2. Novel H6 Transformerless Inverter

Novel H6 transformerless inverter is proposed in this paper to eliminate the leakage current, reduce the conduction loss and increase the efficiency. The circuit for this inverter is shown in Figure 2. As seen in the figure, it is a modification of the H5 inverter circuit with an additional switch S6 between negative terminal of the DC supply and terminal A. The circuit is based on the DC decoupling method. The PV array is disconnected from the grid during the freewheeling modes. This circuit is designed to give a new current path during the active mode of negative half cycle of the grid voltage. Even though the number of switches is increased by one compared to the H5 inverter, it reduces the conduction loss comparatively and also increases the efficiency. The common mode voltage is maintained constant thereby eliminating the leakage current. The detailed analysis of this novel H6

transformerless inverter is given in Section 5. A new modulation technique is developed to realize the circuit and is given in Figure 3. The parameters considered for simulating this inverter are given in Table 1.

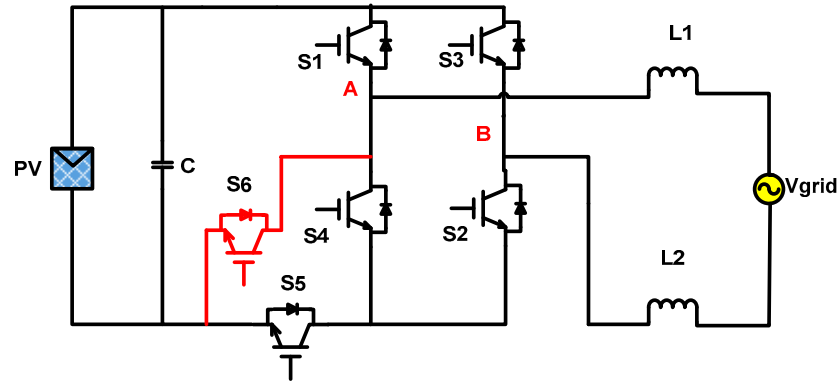


Figure 2. Novel H6 transformerless inverter.

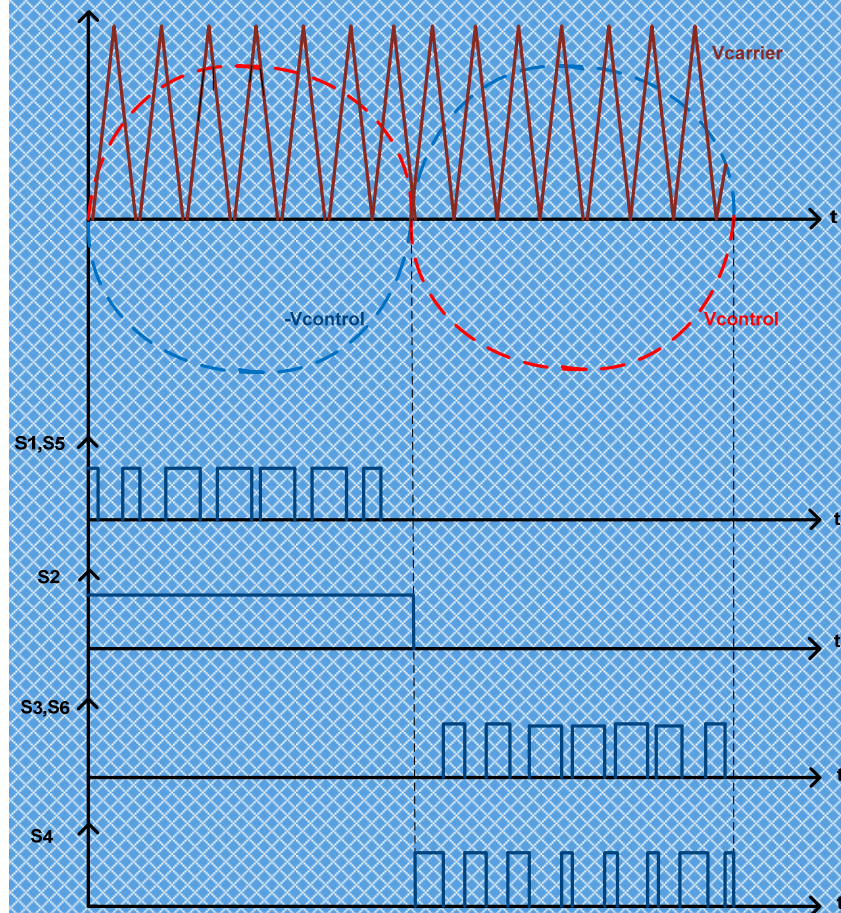


Figure 3. Modulation technique for novel H6 transformerless inverter.

Parasitic capacitance is modelled by two capacitors  $C_{pv1}$  and  $C_{pv2}$  of 1 nF each, connected between the positive and negative terminals of DC supply, respectively, with respect to ground. Symmetrical inductor filter is used in the circuit with inductors of 4.06 mH. The switching frequency is 10 KHz. The switches S1 and S5 operate at switching frequency during the positive half cycle of the grid voltage whereas switches S3 and S6 operate at switching frequency during the negative half cycle of the grid voltage. Switch S2 operates at grid frequency during the positive half cycle of the grid voltage whereas switch S4 operates

complimentary to switch S3 at switching frequency during the negative half cycle of the grid voltage.

**Table 1.** Parameters of the simulation model.

Parameters	Values
Input Voltage	400 V (DC)
Grid Voltage/Frequency	230 V r.m.s./50 Hz
Grid Current	7.07 A
DC bus Capacitor	500 $\mu$ F
Switching Frequency	10 KHz
Filter inductors	$L_1 = L_2 = 4.06$ mH
PV parasitic capacitor	$C_{pv1} = C_{pv2} = 1$ nF
Ground Resistance	5 $\Omega$

### 3. Leakage Current Analysis

Figure 4 indicates the full bridge inverter which is also called H4 inverter with four switches. P and N are the positive and negative terminals of DC supply. A and B are the output terminals of the inverter. The inverter output is fed to the grid through the filter. Additionally, the parasitic capacitance ( $C_{pv}$ ) between the PV and ground is shown in the figure. The expression for common mode voltage ( $V_{cm}$ ) is given by Equation (1) and it is the average of the voltage between output terminals and reference negative terminal.

$$V_{cm} = \frac{V_{AN} + V_{BN}}{2} \quad (1)$$

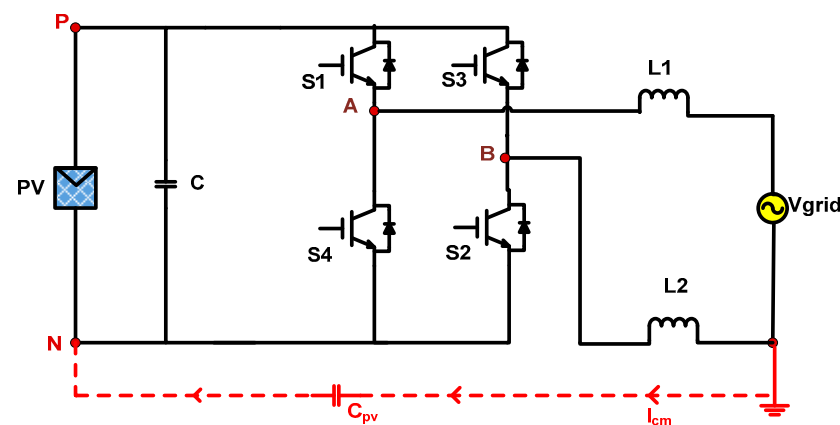


**Figure 4.** Analysis of leakage current in full-bridge (H4) inverter circuit connected to the grid.

Differential mode voltage ( $V_{dm}$ ) is the difference between the inverter output terminals and reference negative terminal. It is given by Equation (2).

$$V_{dm} = V_{AN} - V_{BN} \quad (2)$$

Common mode current ( $I_{cm}$ ) flows due to common mode voltage. The expression for  $I_{cm}$  is given by Equation (3).

$$V_{cm} = C_{pv} \frac{dV_{cm}}{dt} \quad (3)$$

From Equation (3) it is seen that to eliminate common mode current or leakage current, common mode voltage has to be kept constant. Inverter structure and modulation methods decide the values of  $V_{AN}$  and  $V_{BN}$ . Hence, different modulation techniques and inverter topologies are the key to maintain  $V_{cm}$  constant.

Unipolar modulation and bipolar modulation are the commonly used modulation techniques. Unipolar modulation generates three level voltage across the filter and produces low losses. The efficiency generated by the unipolar SPWM technique is high as compared to bipolar modulation. However, due to high frequency common mode voltage, it generates high leakage current.

Bipolar modulation generates two level voltage across the filter and produces high core losses of filter inductors and switching losses. Hence, it has lower efficiency compared to unipolar modulation. However, it generates common mode voltage of constant magnitude and hence the magnitude of leakage current is low.

This paper focuses on the elaborate working of H5, H6 I, H6 II, H6 III inverters and the proposed novel H6 inverter where the DC decoupling network is used. During freewheeling mode, the grid is disconnected from the PV thereby reducing the leakage current to a considerable amount. Unipolar PWM modulation technique is followed to generate the triggering pulses due to its low losses and high efficiency.

#### 4. Performance Analysis of H4, H5 and H6 Inverters

##### 4.1. H4 Inverter

This is the conventional full-bridge inverter with four switches and symmetrical inductors as filter as shown in Figure 5a. During the positive half cycle of the grid voltage, the switches S1 and S2 conduct and the current flows in one direction through the grid. During the negative half cycle of the grid voltage, switches S3 and S4 conduct and the current flows in the reverse direction through the grid. This is shown in Figure 5b,c. Thus, there is a conversion from DC to AC current in the circuit. However, there is no freewheeling path in the circuit which can disconnect the DC supply from the grid. Hence, there are fluctuations in  $V_{cm}$  and there is considerable amount of leakage current.

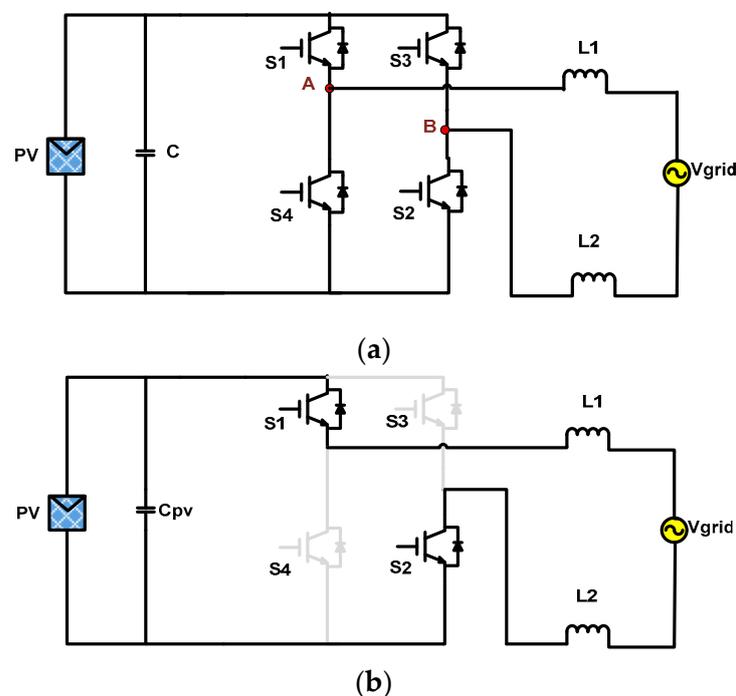
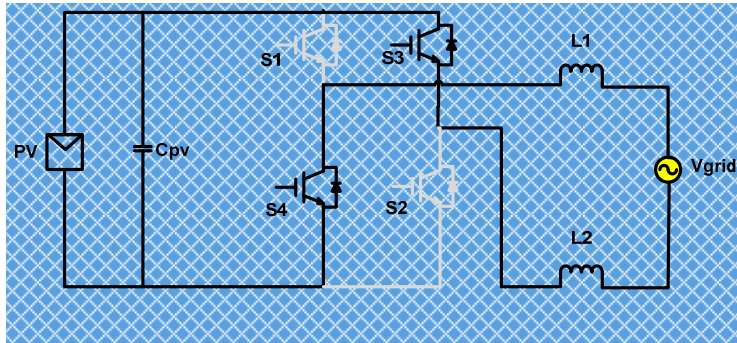


Figure 5. Cont.



**Figure 5.** Full-bridge (H4) inverter connected to the grid. (a) H4 inverter circuit, (b) current conduction during the positive half cycle of grid voltage and (c) current conduction during the negative half cycle of grid voltage.

4.2. H5 Inverter

H5 inverter topology is an improvement to the full-bridge topology with one additional switch on the DC side. Therefore, there are five switches with switch S5 acting similar to a DC decouple unit. Figure 6a shows the H5 inverter circuit connected to the grid. During the positive half cycle of the grid voltage, switch S5, S1 and S2 are on. Letters A and B represent the output terminals of inverter. Thus  $V_{AN} = V_{pv}$  where  $V_{pv}$  is the DC voltage generated by PV panel and  $V_{BN} = 0$ . Therefore,  $V_{cm} = V_{pv}/2$ . The direction of current flow is shown with red arrows. This is shown in Figure 6b. During the freewheeling period, the current freewheels through switch S1 and antiparallel diode of switch S3 as shown in Figure 6c. Therefore,  $V_{AN} = V_{BN} = 0$  and hence  $V_{cm} = 0$ . Switch S5 isolates the DC supply from the grid during freewheeling mode and reduces the leakage current to some extent. Switch S1 always remains on during the conduction and freewheeling period of the positive half cycle of the grid voltage. During the negative half cycle of the grid voltage, switches S5, S3 and S4 are on. Thus  $V_{AN} = 0$  and  $V_{BN} = V_{PV}$ . Therefore,  $V_{cm} = V_{pv}/2$ . This is shown in Figure 6d. During the freewheeling period, the current freewheels through switch S3, grid and antiparallel diode of switch S1 as shown in Figure 6e. Therefore,  $V_{AN} = V_{BN} = 0$  and hence  $V_{cm} = 0$ . Switch S5 once again isolates the DC supply from the grid during freewheeling mode.

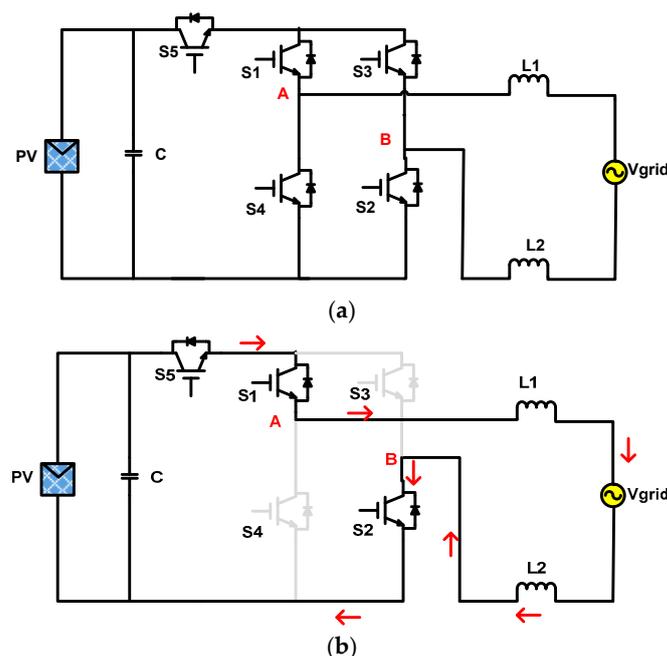


**Figure 6.** Cont.

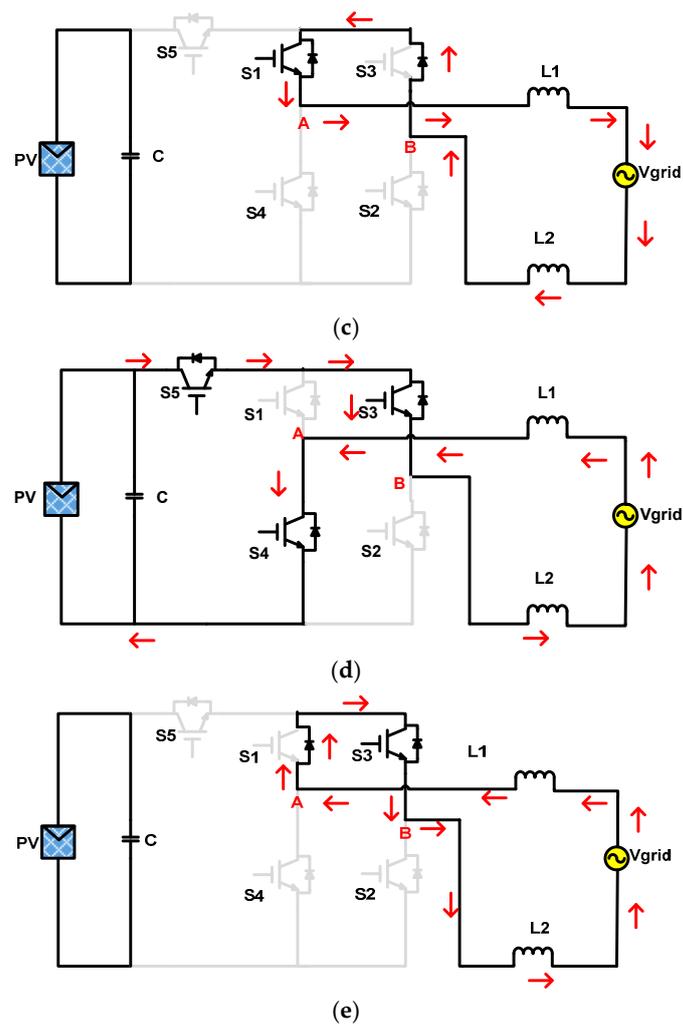


**Figure 6.** H5 inverter and its operating modes. (a) H5 inverter circuit, (b) current conduction during the positive half cycle of the grid voltage, (c) freewheeling mode during the positive half cycle of the grid voltage, (d) current conduction during the negative half cycle of the grid voltage and (e) freewheeling mode during the negative half cycle of the grid voltage.

#### 4.3. H6 I Inverter

As the name suggests, this inverter has six switches in the circuit along with two additional diodes as shown in Figure 7a. During the positive half cycle of the grid voltage, switches S1, S2 and S3 conduct thus connecting the PV to the grid. This is shown in Figure 7b. During the freewheeling period, the current freewheels through switch S2 and diode D1 thereby disconnecting the PV from the grid as can be seen from Figure 7c. During the negative half cycle of the grid voltage, switches S4, S5 and S6 conduct thus connecting the PV to the grid and the current reverses its direction. This is shown in Figure 7d. During the freewheeling period, the current freewheels through switch S5 and diode D2 as can be seen from Figure 7e. Here, switches S2 and S5 operate at grid frequency whereas other switches operate at switching frequency.  $V_{cm}$  remains constant at  $V_m/2$  in all four modes thereby eliminating leakage current from the circuit. The only drawback of this circuit is that three switches conduct during the positive and negative half cycle active modes. This increases the conduction losses and has a negative impact on the efficiency of the inverter circuit.

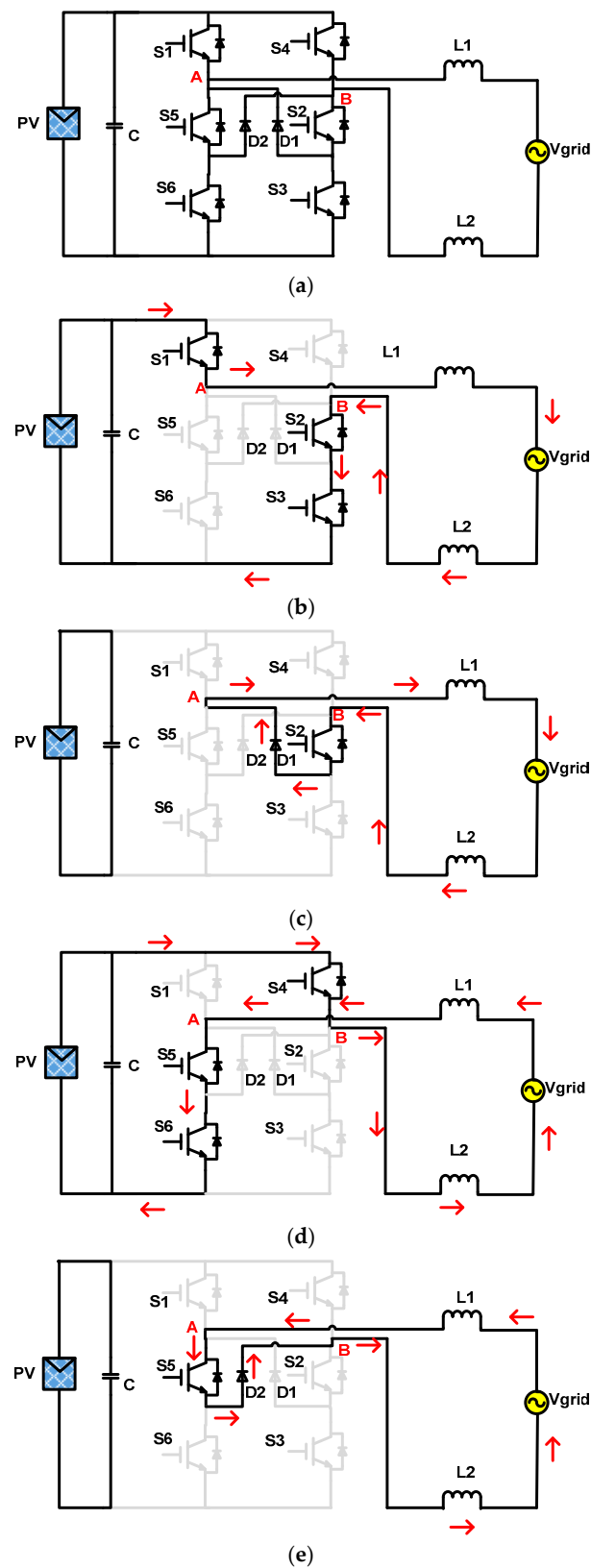


**Figure 7.** H6 I inverter and its operating modes. (a) H6 I inverter circuit, (b) current conduction during the positive half cycle of the grid voltage, (c) freewheeling mode during the positive half cycle of the grid voltage, (d) current conduction during the negative half cycle of the grid voltage and (e) freewheeling mode during the negative half cycle of the grid voltage.

#### 4.4. H6 II Inverter

As shown in Figure 8a, this inverter is a modification of the H5 inverter with an additional switch S6 connected between the positive terminal of DC and terminal B. This inverter was proposed by Li Zang [26] to reduce the conduction loss as compared to the H5 inverter. Switches S1 and S3 operate at grid frequency whereas S2 and S5 operate at switching frequency during the active mode of the positive half cycle of the grid voltage. Switches S4 and S6 also operate at switching frequency during the active mode of the negative half cycle of the grid voltage. During the positive half cycle of the grid voltage, switches S5, S1 and S2 conduct as shown in Figure 8b. During the freewheeling period, S5 is turned off and the current freewheels through antiparallel diode of S3 and switch S1 as shown in Figure 8c. During the negative half cycle of the grid voltage, switches S6 and S4 conduct as shown in Figure 8d. During the freewheeling period, S6 is turned off and current freewheels through the antiparallel diode of S1 and switch S3. This can be seen in Figure 8e. Thus, during the active modes, there are three and two switches conducting, respectively, for the positive and negative half cycles of the grid voltage. It is observed that  $V_{cm}$  remains constant and is equal to  $V_{pv}/2$  in all four modes thereby eradicating the leakage current.

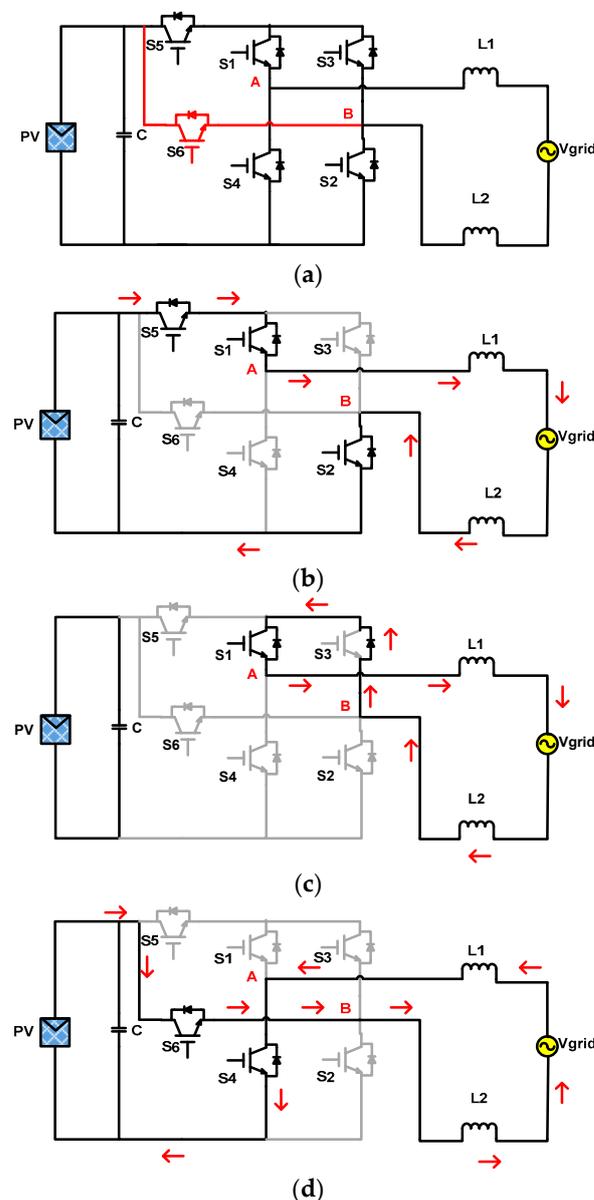
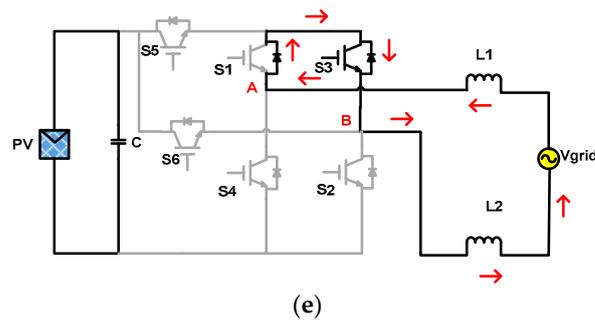


Figure 8. Cont.



**Figure 8.** H6 II inverter and its operating modes. (a) H6 II inverter circuit, (b) current conduction during the positive half cycle of the grid voltage, (c) freewheeling mode during the positive half cycle of the grid voltage, (d) current conduction during the negative half cycle of the grid voltage and (e) freewheeling mode during the negative half cycle of the grid voltage.

#### 4.5. H6 III Inverter

H6 III inverter is seen in Figure 9a. In this inverter circuit, two additional switches S5 and S6 are added symmetrically to the H-bridge inverter. The switches S1 and S4 in one leg of the H-bridge operate at the grid frequency while the switches S3 and S2 commutate at switching frequency. The two additional switches S5 and S6 alternately commute at grid frequency and switching frequency to act as a DC decouple. Accordingly, there are four modes of operation. During the positive half cycle of the grid voltage, switches S5, S1, S2 and S6 conduct as shown in Figure 9b. During the freewheeling period, S2 and S6 are turned off and the current freewheels through the antiparallel diode of S3 and switch S1 as shown in Figure 9c.

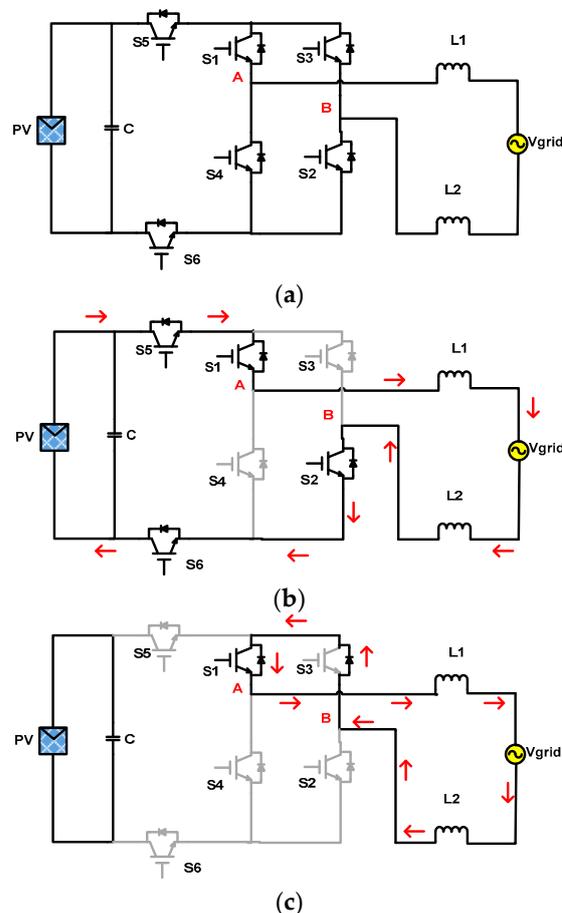


**Figure 9.** Cont.

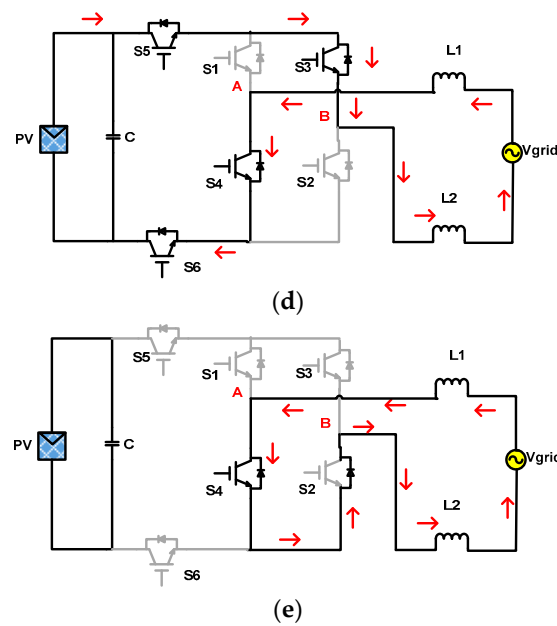


**Figure 9.** H6 III inverter and its operating modes. (a) H6 III inverter circuit, (b) current conduction during the positive half cycle of the grid voltage, (c) freewheeling mode during the positive half cycle of the grid voltage, (d) current conduction during the negative half cycle of the grid voltage and (e) freewheeling mode during the negative half cycle of the grid voltage.

During the negative half cycle of the grid voltage, switches S5, S3, S4 and S6 conduct as shown in Figure 9d. During the freewheeling period, S5 and S3 are turned off and the current freewheels through switch S4 and the antiparallel diode of S2. This can be seen in Figure 9e. Thus, during the active modes, there are four switches conducting for the positive and negative half cycles of the grid voltage. It is observed that  $V_{cm}$  remains constant and is equal to  $V_{pv}/2$  in all four modes thereby eliminating the leakage current.

### 5. Analysis of Proposed Novel H6 Inverter

The circuit for proposed novel H6 inverter was shown in Figure 2. The operation of this proposed novel H6 inverter is as follows. There are four operating modes in each cycle of the grid voltage. Mode I and Mode II are the active mode and freewheeling mode of the positive half cycle of the grid voltage. Mode III and Mode IV are the active mode and freewheeling mode of the negative half cycle of the grid voltage. During the active modes of the grid voltage, the PV array is connected to the grid. During the freewheeling modes of the grid voltage, the PV array is disconnected from the grid. The freewheeling modes facilitate in maintaining the common mode voltage constant which further assists in eliminating the leakage current.

- (a) Mode I: This mode is shown in Figure 10a. It represents the active mode in the positive half cycle of the grid voltage. Switches S1, S2 and S5 are turned on and the other switches are off. The inductor current thus flows through S1, S2 and S5 connecting the PV to the grid. Here,  $V_{AN} = V_{pv}$ ,  $V_{BN} = 0$ . Therefore,  $V_{cm} = (V_{AN} + V_{BN})/2 = V_{pv}/2$ .
- (b) Mode II: This mode is shown in Figure 10b. It represents the freewheeling mode in the positive half cycle of the grid voltage. S2 continues to remain on whereas S1 and S5 is turned off. The inductor current continues to flow in the same direction through S2 and antiparallel diode of S4. Here,  $V_{AN} = V_{BN} = V_{pv}/2$ . Therefore,  $V_{cm} = (V_{AN} + V_{BN})/2 = V_{pv}/2$ .
- (c) Mode III: This mode is shown in Figure 10c. It represents the active mode in the negative half cycle of the grid voltage. S3 and S6 are turned on whereas other switches are off. The inductor current flows through S3 and S6. The conduction losses in

- this mode are less as compared to H5, H6 I and H6 III since only two switches are conducting.  $V_{AN} = 0, V_{BN} = V_{pv}$ . Therefore,  $V_{cm} = (V_{AN} + V_{BN})/2 = V_{pv}/2$ .
- (d) Mode IV: This mode is shown in Figure 10d. It represents the freewheeling mode in the negative half cycle of the grid voltage. Switch S4 is turned on and all other switches are off. The inductor current flows through S4 and antiparallel diode of S2.  $V_{AN} = V_{BN} = V_{pv}/2$ . Therefore,  $V_{cm} = (V_{AN} + V_{BN})/2 = V_{pv}/2$ .

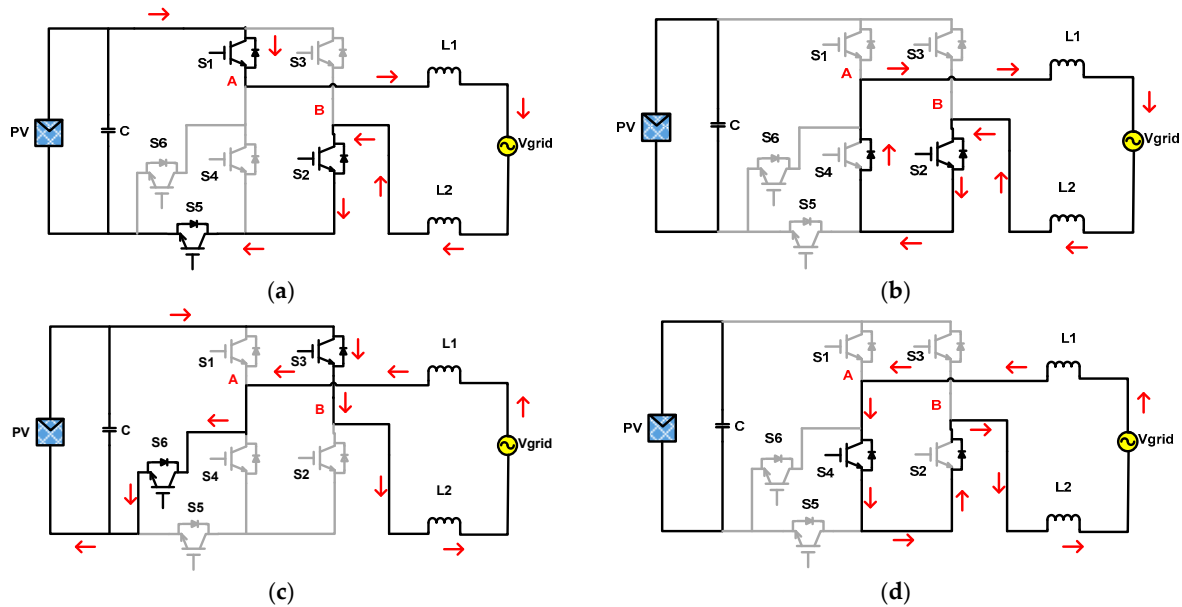


**Figure 10.** Proposed novel H6 inverter operating modes. (a) Current conduction during the positive half cycle of the grid voltage, (b) freewheeling mode during the positive half cycle of the grid voltage, (c) current conduction during the negative half cycle of the grid voltage and (d) freewheeling mode during the negative half cycle of the grid voltage.

It is concluded that  $V_{cm}$  is equal to  $V_{pv}/2$  in all four modes. Hence, this constant  $V_{cm}$  results in nullifying the leakage current in this proposed H6 inverter. Secondly, conduction loss is reduced since only two switches conduct during the active mode of the negative half cycle of the grid voltage. This enhances the efficiency of inverter circuit.

*Control Strategy*

The control strategy employed to generate SPWM pulses is shown in Figure 11.

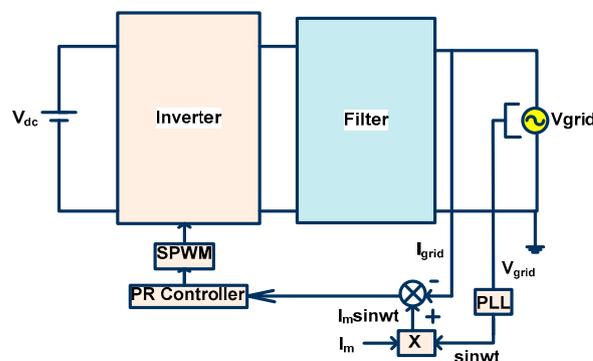


**Figure 11.** Control strategy block diagram.

The grid voltage is sensed and fed to the phase lock loop. Here, SOGI-PLL is employed to generate unity sinusoidal signal which is in phase with the grid voltage. It is multiplied

with reference current and compared with the grid current. A PR controller is employed to get the required output current.

## 6. Simulation Results and Discussion

The simulations of H4, H5, H6 I, H6 II, H6 III inverters and the proposed novel H6 inverter are carried out in MATLAB/Simulink software. The simulations are carried out to compare and analyze the performance of the inverters. The PV module is replaced by 400 V DC source. The grid voltage is considered as 230 V r.m.s at a frequency of 50 Hz.

### 6.1. H4 Simulation Output

The waveforms of  $V_{AN}$ ,  $V_{BN}$ ,  $V_{cm}$  and leakage current of H4 inverter are shown in Figure 12. It can be concluded that the H4 inverter has no freewheeling mode and hence the PV is always connected to the grid. This produces fluctuating common mode voltage and hence there is leakage current flowing from PV to the grid.

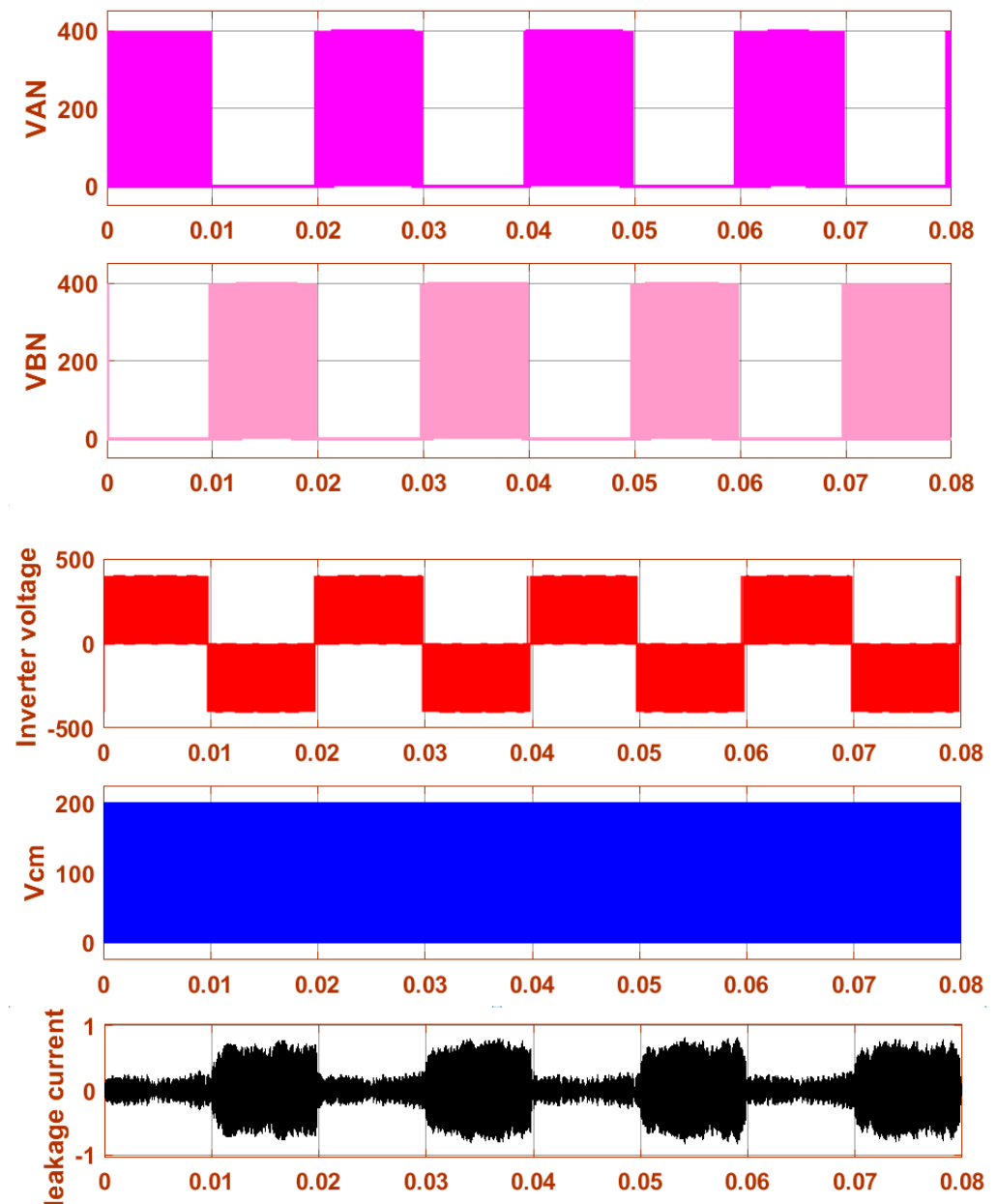


Figure 12. Waveform of  $V_{AN}$ ,  $V_{BN}$ , inverter voltage and  $V_{cm}$ , leakage current of H4 inverter.

### 6.2. H5 Inverter Simulation Output

Figures 12–17 represents the simulation results of H4, H5, H6 I, H6 II, H6 III inverters and the proposed novel H6 inverter, respectively. In the H5 inverter, due to the freewheeling mode, the common mode voltage tries to remain constant thereby reducing the leakage current considerably. This can be seen in Figure 13. However, there are always three switches conducting during each active mode, which increases the conduction losses of the inverter and decreases the efficiency.

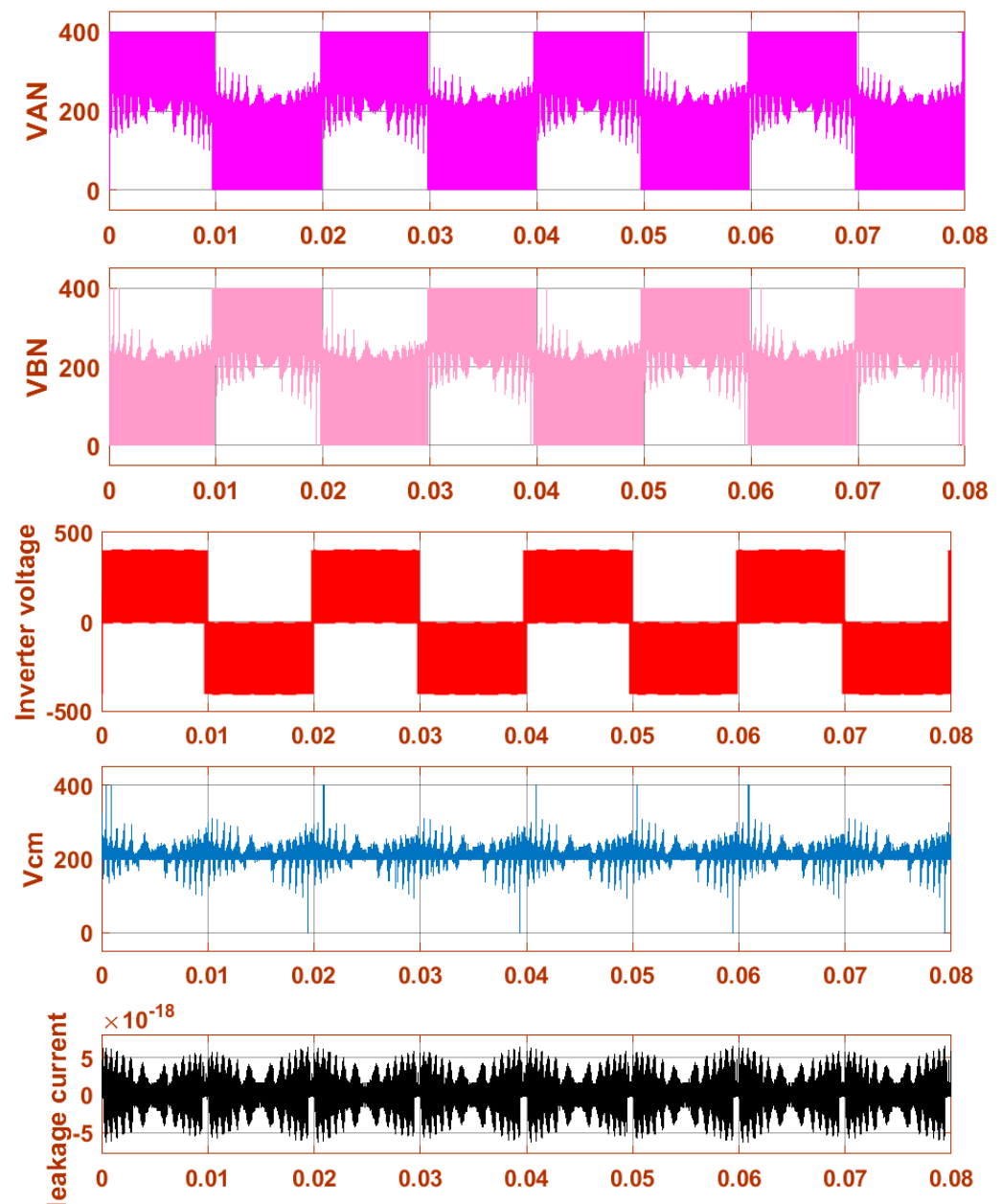


Figure 13. Waveform of  $V_{AN}$ ,  $V_{BN}$ , inverter voltage and  $V_{cm}$ , leakage current of H5 inverter.

### 6.3. H6 I Inverter Simulation Output

In H6 I inverter, the common mode voltage is kept constant and the leakage current is almost zero as can be seen from Figure 14. The performance of H6 I inverter is better than H5 inverter in eliminating leakage current. However, there are also, three switches in this inverter conducting during each active mode, which increases the conduction losses of the inverter and decreases the efficiency.

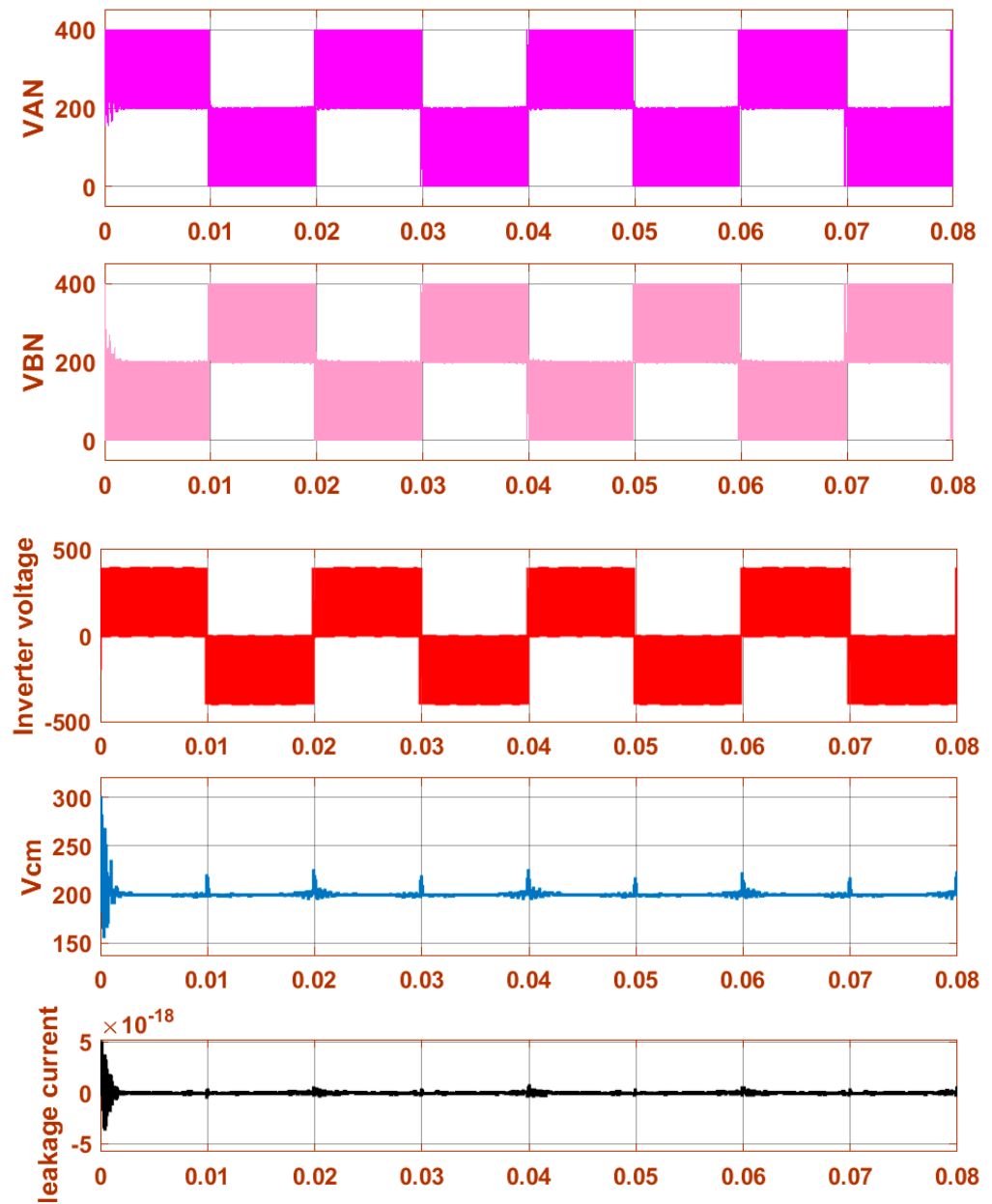
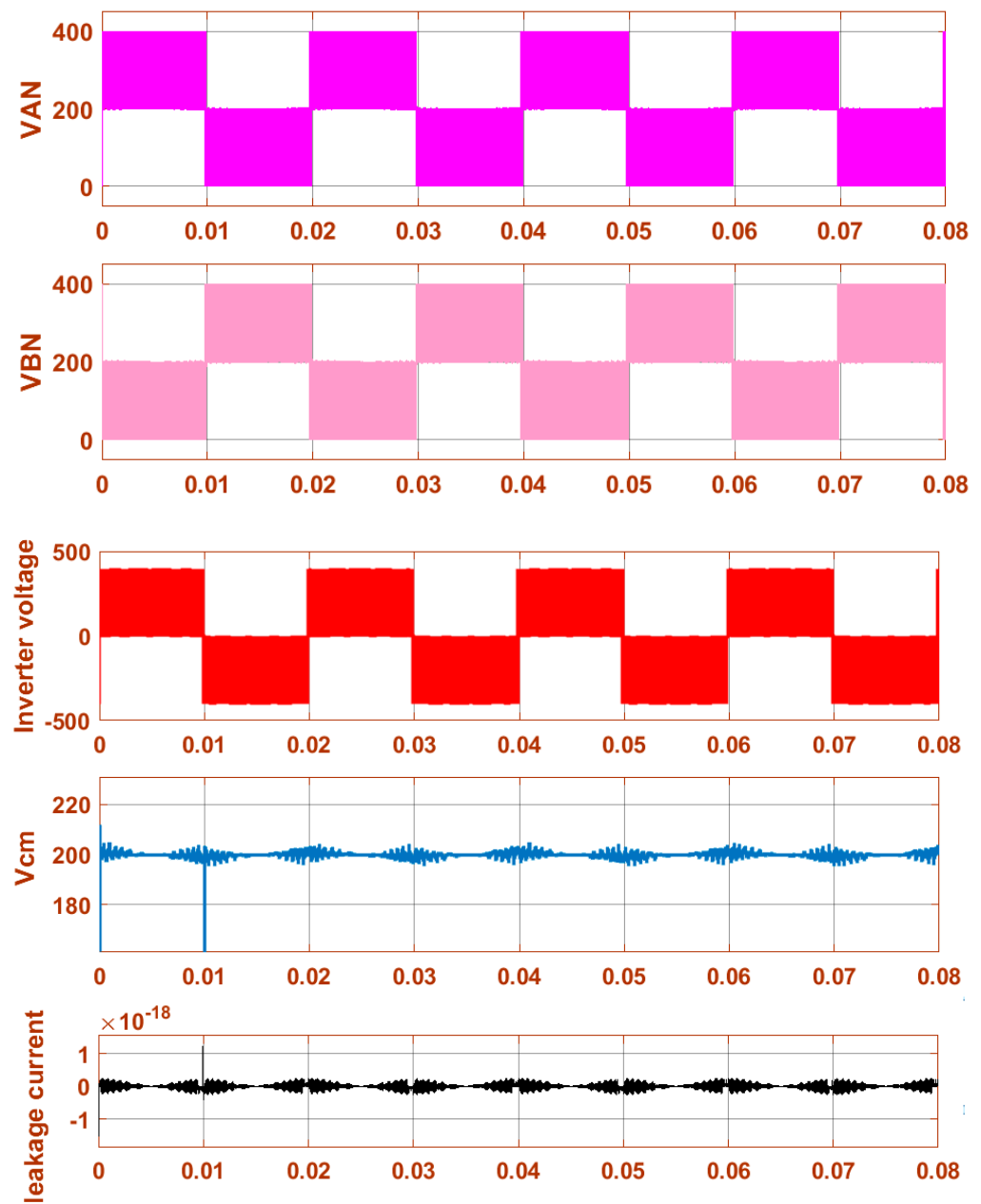


Figure 14. Waveform of  $V_{AN}$ ,  $V_{BN}$ , inverter voltage and  $V_{cm}$ , leakage current of H6 I inverter.

#### 6.4. H6 II Inverter Simulation Output

In the H6 II inverter, the common mode voltage is kept constant and the leakage current is eliminated as can be seen from Figure 15. Additionally, since only two switches are conducting in one of the active modes, the conduction loss is reduced as compared to H5 inverter. This leads to an increase in efficiency.



**Figure 15.** Waveform of  $V_{AN}$ ,  $V_{BN}$ , inverter voltage and  $V_{cm}$ , leakage current of H6 II inverter.

### 6.5. H6 III Inverter Simulation Output

In the H6 III inverter, the common mode voltage is maintained almost constant and the leakage current is reduced to a greater extent as can be seen from Figure 16. However, conduction losses are high since four switches conduct during each active mode.

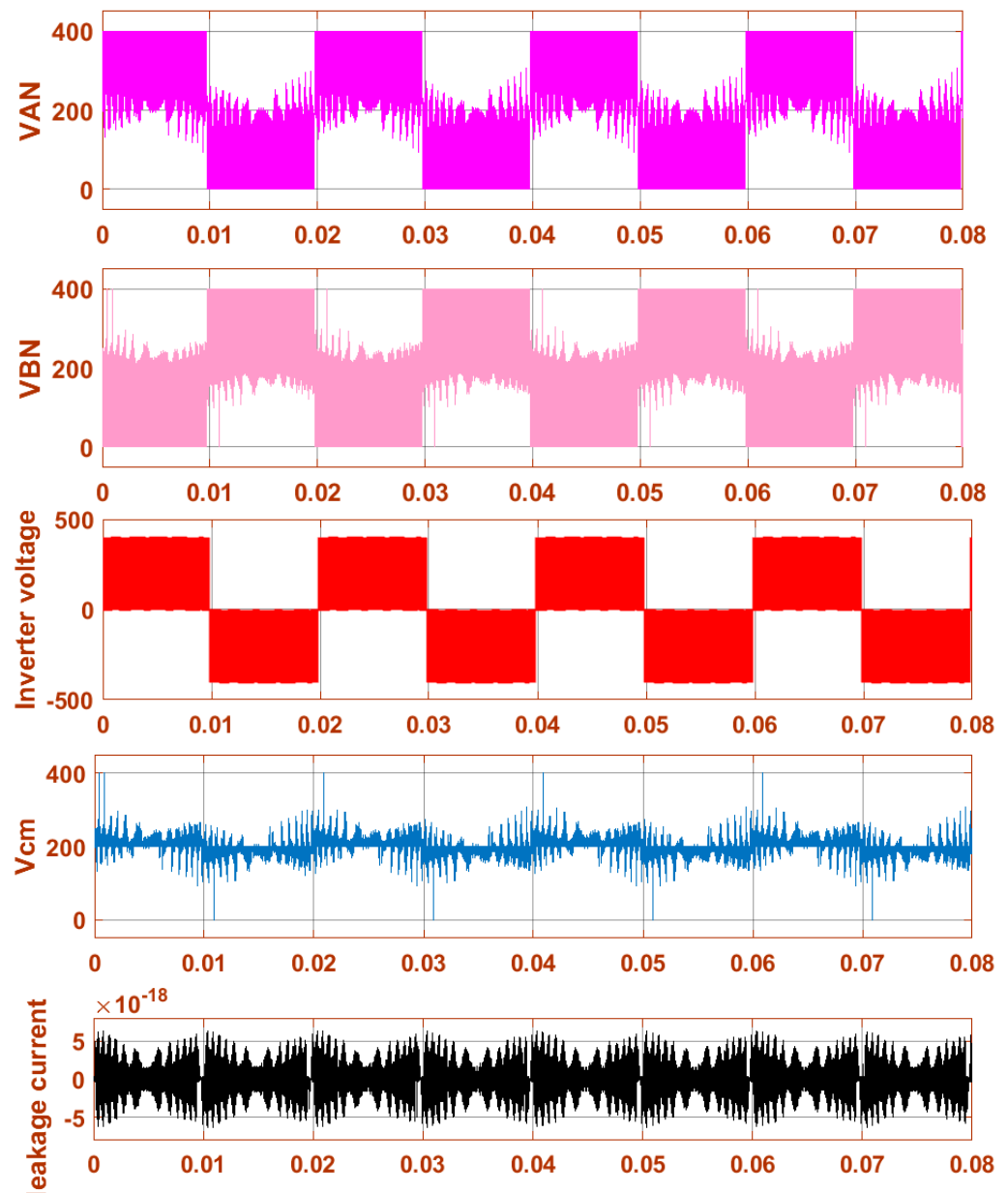
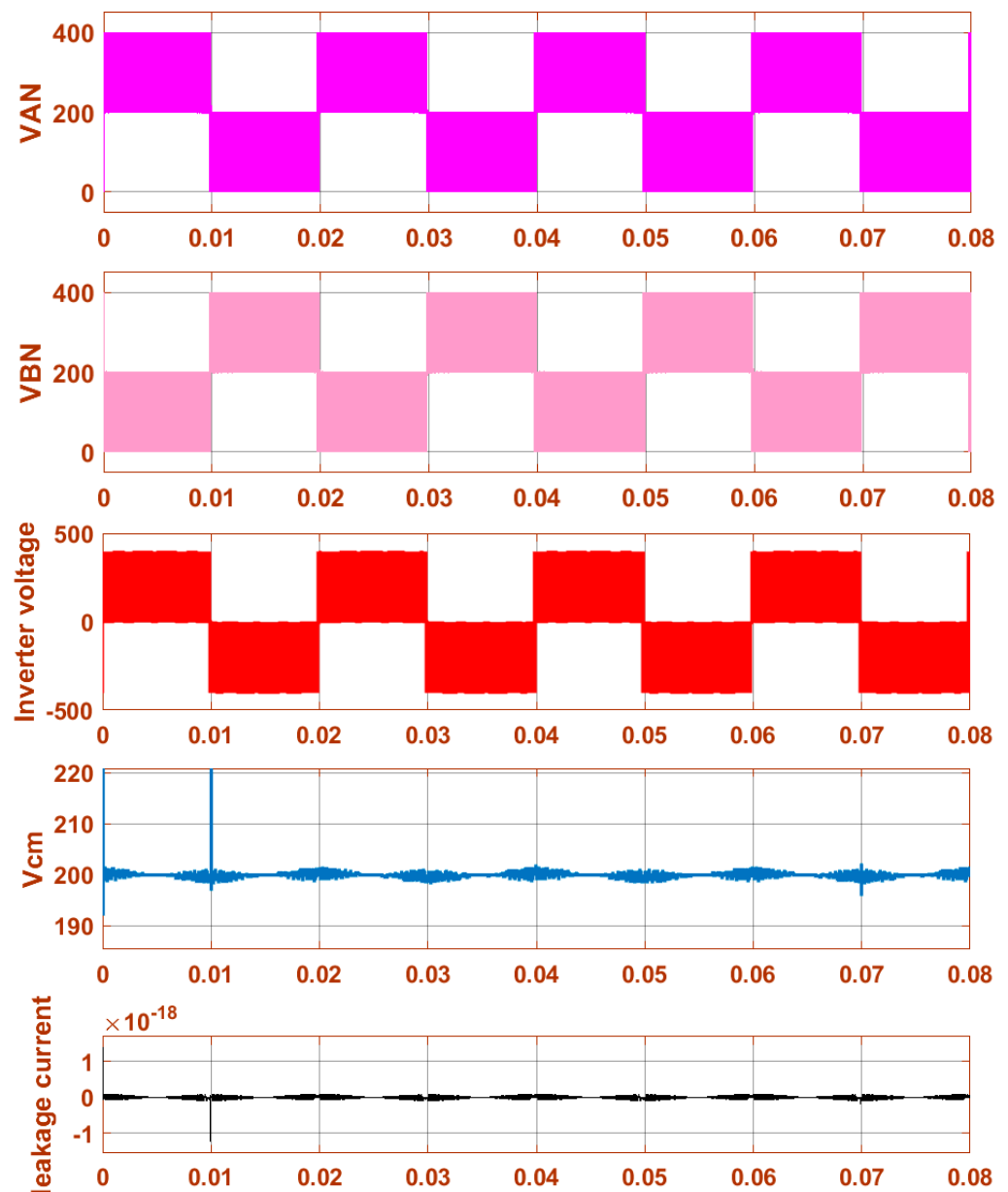


Figure 16. Waveform of  $V_{AN}$ ,  $V_{BN}$ , inverter voltage and  $V_{cm}$ , leakage current of H6 III inverter.

#### 6.6. Proposed Novel H6 Inverter Simulation Output

In the proposed novel H6 inverter, from Figure 17, it can be seen that the common mode voltage is maintained constant and the leakage current is eliminated. Secondly, since only two switches are conducting during one of the active modes, the conduction losses are reduced thereby increasing the efficiency of the inverter. Therefore, comparison between H5, H6 I, H6 II, H6 III inverters and the proposed H6 inverter shows that H6 II and the proposed H6 inverter give better performance in terms of constant common mode voltage and negligible leakage current. Another important aspect of H6 II and the proposed novel H6 inverter is that it produces low conduction loss as compared to the H5, H6 I and H6 III inverters. This is an important feature which enhances the efficiency of the inverter.



**Figure 17.** Waveform of  $V_{AN}$ ,  $V_{BN}$ , inverter voltage and  $V_{cm}$ , leakage current of proposed novel H6 inverter.

A table of comparison of inverters is shown in Table 2 to compare and highlight the performance of the H4, H5, H6 I, H6 II, H6 III inverters and novel H6 inverter based on the total number of switches present in the circuit, switches operating in active mode and freewheeling mode during the positive and negative half cycles of the grid voltage, conduction losses, efficiency, cost and type of decoupling method. HERIC inverter, a widely used inverter due to its high efficiency and reliability, is also compared with H5 and family of H6 inverters along with novel H6 inverter. However, because the HERIC inverter is based on AC decoupling, it is not analyzed in this paper and hence no simulation results are carried out. From the simulation results of the DC-decoupled inverters, it is seen that the novel H6 inverter outperforms the H5, H6 I and H6 III inverters in suppressing the leakage current, reducing conduction loss and enhancing the efficiency. Its performance is on par with the H6 II inverter. The cost of the novel H6 inverter with six switches is more than the H5 inverter with five switches and same as the HERIC inverter. The HERIC inverter gives the best performance in terms of increased efficiency as is proved in the

literature. However, the novel H6 inverter can be considered second best after the HERIC inverter from the simulation results.

**Table 2.** Comparison of inverters.

A	B	C		D		E	F	G	H
		Active Mode	Freewheeling Mode	Active Mode	Freewheeling Mode				
H4	4	2	-	2	-	Less	High	Less	Absent
H5	5	3	1	3	1	More compared to H4, H6 II, HERIC, novel H6	Less compared to H4, H6 II, HERIC, novel H6	Higher than H4 but less than H6 I, H6 II, H6 III, HERIC and novel H6	DC side
H6 I	6	3	1	3	1	High compared to H4, H5, H6 II, HERIC, novel H6	Less compared to H4, H5, H6 II, HERIC, novel H6	High due to 6 switches	DC side
H6 II	6	3	1	2	1	Less compared to H5, H6 I, H6 III	High compared to H5, H6 I, H6 III	High due to 6 switches	DC side
H6 III	6	4	1	4	1	Maximum	Low	High due to 6 switches	DC side
HERIC	6	2	1	2	1	Least	Highest	High due to 6 switches	AC side
Novel H6	6	3	1	2	1	Less compared to H5, H6 I, H6 III	High compared to H5, H6 I, H6 III	High due to 6 switches	DC side

A—Inverter; B—Number of Switches; C—For  $V_g > 0$ , D—For  $V_g < 0$ ; E—Conduction loss; F—Efficiency; G—Cost; H—Decoupling.

## 7. Conclusions

An elaborate analysis of the H4, H5, H6 I, H6 II and H6 III inverters is carried out to minimize the leakage current in a grid connected transformerless inverter circuit. Their performances are compared based on common mode voltage, leakage current, conduction loss and efficiency. It is seen that H5 inverter produces the same conduction loss as H6 I since three switches conduct during the active modes whereas H6 III generates more conduction loss compared to H5, since four switches conduct during the active modes. A novel H6 inverter circuit is proposed in this paper to reduce the conduction loss and enhance the inverter efficiency. This novel H6 inverter maintains constant common mode voltage and hence is responsible for eliminating the leakage current. This is achieved by modifying the H5 topology by inserting one switch between the negative terminal of the PV and the midpoint of the first leg of the bridge circuit.

The simulation results show that the performance of this proposed novel H6 inverter is far superior compared to the conventional H5 topology in suppressing the leakage current even though it uses six switches in the circuit. It reduces the conduction losses compared to the H5 topology due to the direct current path provided by the additional switch. It can also be concluded that the efficiency offered by the proposed novel H6 inverter is higher compared to the conventional H5 inverter. Thus, for a single phase grid connected PV system, the proposed novel H6 inverter can be a promising topology for eliminating leakage current, reducing conduction loss and enhancing the inverter efficiency.

**Author Contributions:** Conceptualization, A.A.D. and S.M.; Methodology, Software and Validation, A.A.D., S.M. and T.S.; Investigation, Resources, Writing—Original Draft Preparation, Writing—Review and Editing, Visualization, Supervision and Project Administration, A.A.D., S.M. and T.S. All authors have read and agreed to the published version of the manuscript.

**Funding:** The authors gratefully acknowledge the support offered by the Science and Engineering Research Board (SERB), Department of Science and Technology, Government of India, under the grant number: EEQ/2021/000294 for this research work.

**Institutional Review Board Statement:** Not applicable.

**Informed Consent Statement:** Not applicable.

**Data Availability Statement:** Not applicable.

**Conflicts of Interest:** The authors declare no conflict of interest.

## Abbreviations

The following abbreviations are used in this manuscript:

$C_{pv}$	Parasitic capacitance between PV and ground
$V_{cm}$	Common mode voltage
$I_{cm}$	Common mode current
$A, B$	Output terminals of inverter
$P, N$	Positive and negative terminals, respectively, of DC supply
$V_{AN}$	Voltage between A and N
$V_{BN}$	Voltage between B and N
$V_{dm}$	Differential mode voltage
$V_{pv}$	DC voltage generated by PV panel
$L_1, L_2$	Filter inductors
$V_g$	Grid voltage

## Nomenclature

PV	Photovoltaics
HERIC	High efficiency and reliable inverter concept
SPWM	Sinusoidal pulse width modulation
HB-ZVR	H bridge zero-voltage state rectifier
BDC	Bidirectional clamping
SOGI-PLL	Second-order generalized integrator–phase lock loop
PR	Proportional resonant

## References

- Gupta, A.K.; Joshi, M.S.; Agarwal, V. Improved Transformerless Grid-Tied PV Inverter Effectively Operating at Twice the Switching Frequency with Constant CMV and Reactive Power Capability. *IEEE J. Emerg. Sel. Top. Power Electron.* **2019**, *8*, 3477–3486. [[CrossRef](#)]
- Khan, M.N.; Forouzes, M.; Siwakoti, Y.P.; Li, L.; Kerekes, T.; Blaabjerg, F. Transformerless Inverter Topologies for Single-Phase Photovoltaic Systems: A Comparative Review. *IEEE J. Emerg. Sel. Top. Power Electron.* **2019**, *8*, 805–835. [[CrossRef](#)]
- Tan, F.; Suan, K.; Rahim, N.A.; Hew, W.P. Modeling, analysis and control of various types of transformerless grid connected PV inverters. In Proceedings of the 2011 IEEE First Conference on Clean Energy and Technology (CET 2011), Kuala Lumpur, Malaysia, 27–29 June 2011; pp. 51–56. [[CrossRef](#)]
- Mathi, A.A.D.; Ramaprabha, R. Comparative Analysis of Grid Connected Transformerless Photovoltaic Inverters for Leakage Current Minimization. *Indian J. Sci. Technol.* **2018**, *11*, 1–8. [[CrossRef](#)]
- Gonzalez, R.; Lopez, J.; Sanchis, P.; Marroyo, L. Transformerless Inverter for Single-Phase Photovoltaic Systems. *IEEE Trans. Power Electron.* **2007**, *22*, 693–697. [[CrossRef](#)]
- Araujo, S.V.; Zacharias, P.; Mallwitz, R. Highly Efficient Single-Phase Transformerless Inverters for Grid-Connected Photovoltaic Systems. *IEEE Trans. Ind. Electron.* **2010**, *57*, 3118–3128. [[CrossRef](#)]
- Kerekes, T.; Teodorescu, R.; Rodriguez, P.; Vazquez, G.; Aldabas, E. A New High-Efficiency Single-Phase Transformerless PV Inverter Topology. *IEEE Trans. Ind. Electron.* **2011**, *58*, 184–191. [[CrossRef](#)]
- Patrao, I.; Figueres, E.; Espin, F.G.; Garcera, G. Transformerless topologies for grid-connected single-phase photovoltaic inverters. *Renew. Sustain. Energy Rev.* **2011**, *15*, 3423–3431. [[CrossRef](#)]
- Hassaine, L.; Olias, E.; Quintero, J.; Salas, V. Overview of power inverter topologies and control structures for grid connected-photovoltaic systems. *Renew. Sustain. Energy Rev.* **2014**, *30*, 796–807. [[CrossRef](#)]
- Li, W.; Gu, Y.; Luo, H.; Cui, W.; He, X.; Xia, C. Topology Review and Derivation Methodology of Single-Phase Transformerless Photovoltaic Inverters for Leakage Current Suppression. *IEEE Trans. Ind. Electron.* **2015**, *62*, 4537–4551. [[CrossRef](#)]
- Islam, M.; Mekhilef, S.; Hasan, M. Single phase transformerless inverter topologies for grid-tied photovoltaic system: A review. *Renew. Sustain. Energy Rev.* **2015**, *45*, 69–86. [[CrossRef](#)]
- Jana, J.; Saha, H.; Bhattacharya, K.D. A review of inverter topologies for single-phase grid-connected photovoltaic systems. *Renew. Sustain. Energy Rev.* **2017**, *72*, 1256–1270. [[CrossRef](#)]
- Ahmad, Z.; Singh, S.N. Comparative analysis of single phase transformerless inverter topologies for grid connected PV system. *Sol. Energy* **2017**, *149*, 245–271. [[CrossRef](#)]

14. Zeb, K.; Uddin, W.; Khan, M.A.; Ali, Z.; Ali, M.U.; Christofides, N.; Kim, H.J. A comprehensive review on inverter topologies and control strategies for grid connected photovoltaic system. *Renew. Sustain. Energy Rev.* **2018**, *94*, 1120–1141. [[CrossRef](#)]
15. Zhang, L.; Sun, K.; Feng, L.; Wu, H.; Xing, Y. A Family of Neutral Point Clamped Full-Bridge Topologies for Transformerless Photovoltaic Grid-Tied Inverters. *IEEE Trans. Power Electron.* **2013**, *28*, 730–739. [[CrossRef](#)]
16. Ahmad, Z.; Singh, S.N. An improved single phase transformerless inverter topology for grid connected PV system with reduce leakage current and reactive power capability. *Sol. Energy* **2017**, *157*, 133–146. [[CrossRef](#)]
17. Islam, M.; Mekhilef, S. H6-type transformerless single-phase inverter for grid-tied photovoltaic system. *IET Power Electron.* **2015**, *8*, 636–644. [[CrossRef](#)]
18. Freddy, T.K.S.; Lee, J.-H.; Moon, H.-C.; Lee, K.-B.; Rahim, N.A. Modulation Technique for Single-Phase Transformerless Photovoltaic Inverters With Reactive Power Capability. *IEEE Trans. Ind. Electron.* **2017**, *64*, 6989–6999. [[CrossRef](#)]
19. Albalawi, H.; Zaid, S.A. An H5 Transformerless Inverter for Grid Connected PV Systems with Improved Utilization Factor and a Simple Maximum Power Point Algorithm. *Energies* **2018**, *11*, 2912. [[CrossRef](#)]
20. Anurag, A.; Deshmukh, N.; Maguluri, A.; Anand, S. Integrated DC–DC Converter Based Grid-Connected Transformerless Photovoltaic Inverter With Extended Input Voltage Range. *IEEE Trans. Power Electron.* **2018**, *33*, 8322–8330. [[CrossRef](#)]
21. Kuncham, S.K.; Annamalai, K.; Nallamothu, S. A new structure of single-phase two-stage hybrid transformerless multilevel PV inverter. *Int. J. Circ. Appl.* **2018**, *47*, 152–174. [[CrossRef](#)]
22. Li, H.; Zeng, Y.; Zhang, B.; Zheng, Q.; Hao, R.; Yang, Z. An Improved H5 Topology with Low Common Mode Current for Transformerless PV Grid Connected Inverter. *IEEE Trans. Power Electron.* **2018**, *34*, 1254–1256. [[CrossRef](#)]
23. Siwakoti, Y.P.; Blaabjerg, F. Common-Ground-Type Transformerless Inverters for Single-Phase Solar Photovoltaic Systems. *IEEE Trans. Ind. Electron.* **2018**, *65*, 2100–2111. [[CrossRef](#)]
24. Xu, M.; Zhang, L.; Xing, Y.; Feng, L. A Novel H6-Type Transformerless Inverter for Grid-Connected Photovoltaic Application. In Proceedings of the 7th IEEE Conference on Industrial Electronics and Applications (ICIEA 2012), Singapore, 18–20 July 2012; pp. 58–63. [[CrossRef](#)]
25. Yang, B.; Li, W.; Gu, Y.; Cui, W.; He, X. Improved Transformerless Inverter with Common-Mode Leakage Current Elimination for a Photovoltaic Grid-Connected Power System. *IEEE Trans. Power Electron.* **2012**, *27*, 752–762. [[CrossRef](#)]
26. Zhang, L.; Sun, K.; Xing, Y.; Xing, M. H6 Transformerless Full-Bridge PV Grid-tied Inverters. *IEEE Trans. Power Electron.* **2014**, *29*, 1229–1238. [[CrossRef](#)]
27. Datta, A.; Bhattacharya, G.; Mukherjee, D.; Saha, H. Ground Leakage Current Elimination in a Transformerless Unipolar Modulation Based Single Phase Grid-Connected Photovoltaic System. In Proceedings of the IEEE PES Asia-Pacific Power and Energy Engineering Conference (APPEEC), Hong Kong, China, 8–11 December 2013. [[CrossRef](#)]
28. Kumar, K.S.; Kirubakaran, A.; Subrahmanyam, N. Bidirectional Clamping-Based H5, HERIC, and H6 Transformerless Inverter Topologies With Reactive Power Capability. *IEEE Trans. Ind. Appl.* **2020**, *56*, 5119–5128. [[CrossRef](#)]
29. Ahmad, S.; Mekhilef, S.; Mokhlis, H. A grid-tied photovoltaic transformer-less inverter with reduced leakage current. *IOP Conf. Ser. Earth Environ. Sci.* **2021**, *673*, 012016. [[CrossRef](#)]
30. Gaafar, M.A.; Orabi, M.; Ibrahim, A.; Kennel, R.; Abdelrahem, M. Common-Ground Photovoltaic Inverters for Leakage Current Mitigation: Comparative Review. *Appl. Sci.* **2021**, *11*, 11266. [[CrossRef](#)]